

Out-of-equilibrium states and quasi-many-body localization in polar lattice gases

L. Barbiero,¹ C. Menotti,² A. Recati,^{2,3} and L. Santos⁴

¹Dipartimento di Fisica e Astronomia “Galileo Galilei”, Università di Padova, 35131 Padova, Italy

²INO-CNR BEC Center and Dipartimento di Fisica, Università di Trento, 38123 Povo, Italy

³Technische Universität München, James-Frank-Strasse 1, 85748 Garching, Germany

⁴Institut für Theoretische Physik, Leibniz Universität Hannover, Appelstrasse 2, DE-30167 Hannover, Germany

(Received 15 May 2015; revised manuscript received 29 June 2015; published 9 November 2015)

The absence of energy dissipation leads to an intriguing out-of-equilibrium dynamics for ultracold polar gases in optical lattices, characterized by the formation of dynamically bound on-site and inter-site clusters of two or more particles, and by an effective blockade repulsion. These effects combined with the controlled preparation of initial states available in cold-gas experiments can be employed to create interesting out-of-equilibrium states. These include quasiequilibrated effectively repulsive 1D gases for attractive dipolar interactions and dynamically bound crystals. Furthermore, nonequilibrium polar lattice gases can offer a promising scenario for the study of quasi-many-body localization in the absence of quenched disorder. This fascinating out-of-equilibrium dynamics for ultracold polar gases in optical lattices may be accessible in on-going experiments.

DOI: 10.1103/PhysRevB.92.180406

PACS number(s): 67.85.-d, 03.75.Lm, 05.30.Jp, 75.10.Pq

Out-of-equilibrium dynamics of isolated quantum systems has recently attracted major interest [1,2], in particular in the context of ultracold gases, where dissipation is basically absent [3]. Nonequilibrium quantum dynamics constitutes an exciting new field, notably in what concerns many-body localization (MBL), i.e., localization in excited states of interacting many-body systems [4]. Recent cold-gas experiments are starting to unveil the nontrivial physics of MBL [5].

Although MBL is typically discussed in the presence of disorder, localization may occur in the absence of it, as first discussed for ³He diffusion in ⁴He crystals [6,7]. Beyond a critical concentration, immobile ³He clusters could lead to percolation for the remaining ³He atoms. Quasi-MBL and glassy dynamics without disorder are attracting growing attention, and various mechanisms for localization and eventual delocalization have been discussed [8–15].

Meanwhile, experiments on magnetic atoms [16–18] and polar molecules [19–21] are starting to reveal the fascinating physics of dipolar gases. These gases are markedly different from their nondipolar counterparts due to the long-range anisotropic character of the dipole-dipole interaction (DDI) [22,23]. Polar gases in optical lattices (OLs) offer exciting possibilities for the study of lattice models [23] and quantum magnetism [24,25].

In this Rapid Communication, we study nonequilibrium dynamics of 1D polar lattice gases. This dynamics is characterized by dynamically bound on-site and inter-site clusters (BCs) generalizing on-site repulsively bound pairs in nonpolar gases [26–28], and by blockade repulsion (BR). We show how these effects result in interesting out-of-equilibrium states, including repulsive gases with attractive DDI and dynamically bound crystals. Moreover, polar lattice gases allow for quasi-MBL without disorder, as we illustrate for the setup of Fig. 1. These scenarios can be realized in current experiments on polar molecules in OLs.

a. Model. We consider polar bosons in a 1D OL. For a deep lattice the system is described by the extended Bose-Hubbard model (EBHM) [22,23]

$$H = -J \sum_{\langle ij \rangle} \hat{b}_i^\dagger \hat{b}_j + \frac{U}{2} \sum_i \hat{n}_i (\hat{n}_i - 1) + V \sum_{i,r>0} \frac{\hat{n}_i \hat{n}_{i+r}}{r^3}, \quad (1)$$

where $\langle \dots \rangle$ denotes nearest neighbor (NN), b_i (b_i^\dagger) destroys (creates) bosons at the i th site, $n_i = b_i^\dagger b_i$, J is the hopping rate, U characterizes the combined on-site short-range interactions and DDI, and V/r^3 is the strength of the DDI between sites placed $r \geq 1$ sites apart. J , U , and V can be tuned independently by changing the lattice depth, the transverse confinement [29], and the orientation and strength of the polarizing field ($V < 0$ for polarization along the lattice axis), and by Feshbach resonances.

b. Bound pairs. We revisit first the concept of bound pairs in nonpolar gases ($V = 0$). Doubly occupied sites are characterized by an interaction energy U . If $|U| \gg J$, energy conservation maintains on-site pairs irrespective of the sign of U [30]. For $U > 0$ those pairs, also called repulsively bound pairs [27], are hence dynamically bound. Conversely, two separated particles cannot be brought to the same site; i.e., singlons experience hard-core repulsion [31]. However, singlons may resonantly move through on-site pairs since a single-particle hopping swaps doublon and singlon positions ($21 \rightarrow 12$) [32,33].

The long-range DDI allows for dynamically bound inter-site pairs [34]. Figure 2(a) depicts a typical two-particle spectrum, for $U = 0$ and $V = -100J$. For each center-of-mass quasimomentum $K \in [-\pi, \pi]$, the spectrum presents a continuum of scattering states and a discrete set of isolated inter-site bound states (BSs) [35,36], which as for on-site bound pairs in nonpolar gases are maintained by energy conservation, irrespective of the sign of V . Figures 2(b)–2(d) show the probability of finding two particles r sites apart for the BSs at $K = 0$. For binding energies close to the continuum, the relative position of the pair delocalizes over many sites [Fig. 2(b)]. These delocalized BSs are for any practical purposes indistinguishable from the scattering states. Instead, as shown in Figs. 2(c) and 2(d), deeper BSs present a well defined relative distance r . Below we restrict the term bound pair (BP) to deep BSs at fixed $r \leq r_c$, where the critical r_c is defined as the largest r satisfying the condition $f(r) = 2(J/V)^2/[r^{-3} - (r+1)^{-3}]^2 \ll 1$ [37]. Note that even if $U = 0$, the inter-site DDI stabilizes an on-site BP that is buried within the scattering states in Fig. 2(a), close to

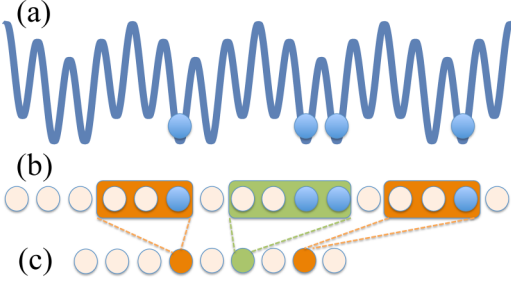


FIG. 1. (Color online) (a) A dimerized lattice can be used to create a gas of singlons and dynamically bound NN dimers; (b) due to the BR a NN dimer (singlon) forms a block $D \equiv 0011$ ($S \equiv 001$); (c) effective lattice formed by the blocks D , S , and additional empty sites. This effective lattice is employed in model (2) to show the realization of quasi-MBL.

energies $E = U = 0$. On-site and NN BPs demand $|V - U| \gg J$ to avoid resonances between on-site and inter-site interactions [38].

c. Bound clusters. On-site interactions may bind more than two particles in on-site BCs. However, on-site BCs are unstable against three-body losses and play a relevant role only at relatively large lattice fillings [39]. Polar lattice gases allow for inter-site BCs of more than two particles, each particle being within a distance $r \leq r_c$ of at least another particle of the cluster. Several important points must be noted. First, although sites with more than one particle may be involved, inter-site BCs are typically formed by singly occupied sites, and hence these clusters are in general stable against three-body losses. Second, whereas on-site BPs are obviously precluded for polarized Fermi gases, inter-site BPs and BCs are possible even in that case. Third, in contrast to on-site BCs, inter-site BCs may present internal resonances; e.g., the cluster 1101 may remain bound, but resonates with 1011. BCs are a general

feature of nonequilibrium polar lattice gases in any dimension even at low fillings, as long as the DDI is large enough. In particular, massive BCs of a size comparable to the whole system may be formed if the mean-interparticle distance $R < r_c$. An example of massive BC is provided by particles initially placed at regular distances $r_{\text{in}} \leq r_c$. The absence of dissipation maintains this *dynamically bound crystal* [Fig. 3(a)].

d. Blockade repulsion. The formation of inter-site BPs has as a counterpart a vanishing probability of finding the particles at a distance $r \leq r_c$ in loose inter-site BSs and scattering states ($r_c = 2$ for Fig. 2(b) [37]). This exclusion region leads to an effective BR between particles initially at a distance $r_{\text{in}} > r_c$. This BR becomes evident in the density-density correlation $g_2(t, r) = \langle n_i(t)n_{i+r}(t) \rangle / [\langle n_i(t) \rangle \langle n_{i+r}(t) \rangle]$. If $r_{\text{in}} > r_c$ at $t = 0$, the subsequent dynamics shows BR, i.e., $g_2(t > 0, 0 < r \leq r_c) = 0$, as discussed below.

e. Repulsive gas for attractive DDI. Combining BR with a proper initial-state preparation allows for the creation of a repulsive gas for attractive DDI. Such a gas may be realized by placing particles at the minima of a superlattice with period $r_{\text{in}} > r_c$ and subsequently removing the superlattice; atoms in sites with more than two particles may be eliminated by using resonant light [40]. Under these conditions no BP or BC is present, and the system forms a singlon gas with effective BR at radius r_c . We have performed time-dependent density-matrix renormalization group (t-DMRG) simulations [41] for $V = -100J$ and $U = 0$ ($r_c = 2$) and 4 particles initially $r_{\text{in}} = 5$ sites apart. After a short time $\sim J^{-1}$, the density $\langle n_j \rangle$ and $g_2(r = 0)$ converge to the values expected for a homogeneous gas [inset of Fig. 3(b)] [42]. However, due to BR, $g_2(t, 0 < r \leq r_c) = 0$ for all t , whereas $g_2(t, r > r_c)$ has a nontrivial dynamics reaching quasiequilibrium [Fig. 3(b)]. The time-averaged single-particle correlation $\bar{g}_1(r) = \frac{1}{t_2 - t_1} \int_{t_1}^{t_2} dt \langle b_i^\dagger b_{i+r} \rangle(t)$, shown for different times $t_{1,2}$ in Fig. 3(c), also indicates quasiequilibrium. The equilibration of \bar{g}_1 and g_2 relies on the absence of BPs or BCs, contrasting with the quasi-MBL scenario below.

Although the effective repulsive 1D gas resembles a super-Tonks gas [43], the physics behind is very different. In the super-Tonks case, an initially repulsive gas is dynamically brought into an attractive regime. Even if in that regime the two-body ground state is a bound state, in the absence of dissipation the system remains in an excited state characterized by interparticle repulsion. In contrast, BR is crucially maintained by both the absence of dissipation and by the lattice, which provides a finite bandwidth and discrete particle motion.

f. Quasi-many-body localization. Polar lattice gases offer interesting possibilities for the study of quasi-MBL without disorder. BCs of M particles move as a whole with hopping $J(J/V)^{M-1}$, and hence BCs with $M \gg 1$ are for any practical purposes immobile (although in-cluster quasiresonances may be still possible). As for ^3He [6,7], massive BCs and BR may induce percolation for large-enough filling and $|V|/J$. Interestingly, as shown below, 1D polar lattice gases may present quasi-MBL even for low fillings ($R \gg r_c$) and moderate DDI achievable in experiments.

We illustrate the possibilities of 1D polar lattice gases for quasi-MBL within a simplified scenario. Resembling the recent experiment of Ref. [5] we consider a dimerized OL such that only the lower sites are populated [Fig. 1(a)]. After

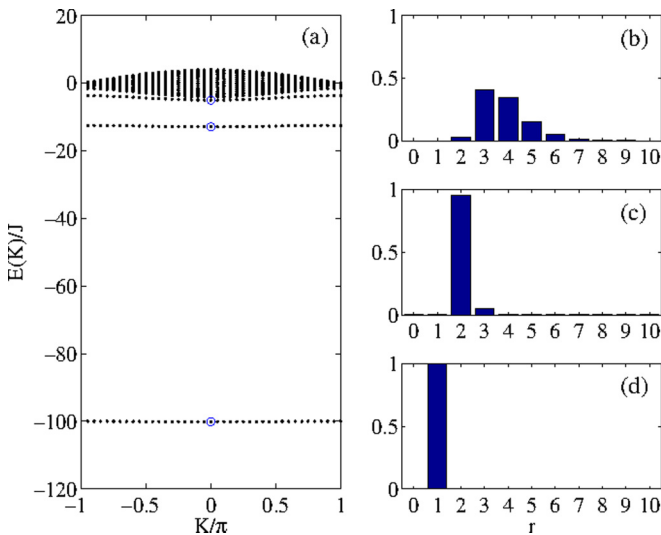


FIG. 2. (Color online) (a) Energy spectrum as a function of the center-of-mass quasimomentum K for two particles in 40 sites for $U = 0$ and $V = -100J$; density of the bound states as a function of the relative coordinate r for the three bound states at $K = 0$, as marked by the blue circles in panel (a), at energies $E/J \approx -5$ (b), -13 (c), and -100 (d).

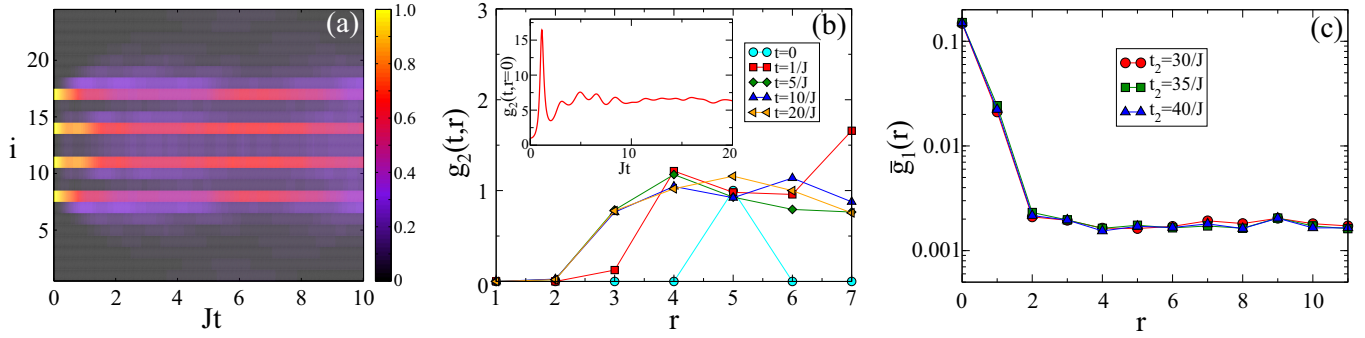


FIG. 3. (Color online) (a) Dynamically bound crystal: density $\langle n_i \rangle$ (obtained using t-DMRG) for $U = 0$ and $V = -100J$ ($r_c = 2$), for 4 particles in 24 sites initially placed $r_{\text{in}} = 3$ sites apart. Note that since $r_{\text{in}} = r_c + 1$, there is still some residual dynamics. For smaller $r_{\text{in}} \leq r_c$ the crystal is perfectly preserved in this time scale. (b)–(c) Effective repulsive 1D gas: same parameters as in panel (a) but $r_{\text{in}} = 5$: (b) $g_2(t, r > 0)$ at different times (in the inset we show $g_2(t, r = 0)$ [42]) and (c) $\bar{g}_1(r)$, for $J(t_2 - t_1) = 5$ and different t_2 values. For both \bar{g}_1 and g_2 , r denotes the distance from an initially occupied site. Note that not only the on-site density and density fluctuations converge to quasiequilibrium, but also \bar{g}_1 and g_2 at longer distances. Note as well that $g_2(t, 0 < r \leq r_c) = 0$ due to BR.

eliminating atoms in doubly occupied sites [40], neighboring lower sites are hence either both occupied, or only one of them, or none. Then the superlattice is removed. We consider $|V|/J$ such that $r_c = 2$, and hence NN dimers form a BP, and a BR at $r_c = 2$ is established. As a result, blocks 0011 and 001 behave as well-defined particles that we call D and S, respectively [Fig. 1(b)]. We neglect DDI for $r > r_c$ neighbors, since it is well within the bandwidth, and obtain the effective model [44]:

$$\hat{H}_{\text{eff}} = - \sum_{\langle ij \rangle} (J \hat{S}_i^\dagger \hat{S}_j + J_D \hat{D}_i^\dagger \hat{D}_j + \Omega \hat{D}_i^\dagger \hat{S}_j^\dagger \hat{S}_i \hat{D}_j), \quad (2)$$

where i, j denote the sites of the effective lattice formed by D's, S's, and empty sites of the original lattice belonging neither to a D nor an S [Fig. 1(c)]. In \hat{H}_{eff} , \hat{D}_j (\hat{S}_j) destroys a D (S) at the effective site j . Assuming for simplicity $U \gg V, J$, the D hopping rate is $J_D = \frac{8}{7} \frac{J^2}{V}$. The third term in \hat{H}_{eff} is the swap $DS \leftrightarrow SD$, occurring at rate $\Omega = \frac{4}{3} \frac{J^2}{V}$. Note that a site of the effective lattice is occupied by a D, an S, or empty. Due to this hard-core constraint, in absence of swapping, D's and S's would trivially localize each other, for any ratio J_D/J .

Swapping allows for the motion of D's and S's. However, the fact that $J_D, \Omega \ll J$ for $J/|V| \ll 1$ may result in localization following arguments similar to those in Ref. [9]. For $J/|V| \rightarrow 0$, the motion of S's is blocked by D's. For finite $J/|V| \ll 1$, the motion of D's changes the energy of the S gas [45]. If this change $\Delta E \gg J_D, \Omega$, the motion of D's is hindered. However, limited quasisonant D mobility, involving $\Delta E < J_D, \Omega$, remains possible, leading to partial D diffusion at times $\sim 1/\Omega$.

We have performed exact diagonalization calculations with periodic boundary conditions (PBC) of the evolution of the many-body state $|\Psi(t)\rangle$ given by model (2) for small systems (n_D, n_S, L) of n_D D's, n_S S's, and L lattice sites, corresponding to $L_{\text{eff}} = L - 3n_D - 2n_S$ effective sites [44]. We average over various initial random distributions of D's and S's at fixed positions in the effective lattice. Figure 4 shows for $\Omega/J = 0.013$ ($V = -100J$) the dynamics of the inhomogeneity of D's, $\Delta N \equiv \frac{1}{L_{\text{eff}}} \sum_{j=1}^{L_{\text{eff}}} |(\Psi(t)|\hat{N}_j - \hat{N}_{j+1}|\Psi(t))|^2$ (with $\hat{N}_j \equiv \hat{D}_j^\dagger \hat{D}_j$) [9]. Perfect homogeneity means $\Delta N = 0$. In Fig. 4 we depict for comparison the results for $\Omega/J = 0.13$ [46].

Whereas for $\Omega/J = 0.13$, D's diffuse within a time scale $1/\Omega$, for $\Omega/J = 0.013$ quasisonances allow only a fraction of D's to delocalize in this time scale (shaded region in Fig. 4) and a much slower dynamics follows. This slow dynamics is characteristic of systems with PBC due the collective motion of all D's [10]. Consistent with this, the time scale of the slow D dynamics for the $(n_D, n_S, L) = (3, 3, 27)$ case is approximately 10 times longer than that for $(2, 2, 20)$ [47]. We hence expect an exponentially diverging time scale for the slow dynamics for growing number of dimers.

We may expand $|\Psi(t)\rangle = \sum_{v=1}^{n_{\text{max}}} \psi(v, t) |v\rangle$ over the $n_{\text{max}} = \binom{L_{\text{eff}}}{n_D + n_S} \binom{n_D + n_S}{n_S}$ many-body states $|v\rangle$ accounting for all possible distributions of S's and D's in the effective lattice. MBL may be visualized as localization in this many-body space. The latter is best quantified by the inverse participation ratio (IPR), $\eta(t) \equiv \frac{1}{n_{\text{max}}} [\sum_v |\psi(v; t)|^4]^{-1}$; a fully delocalized

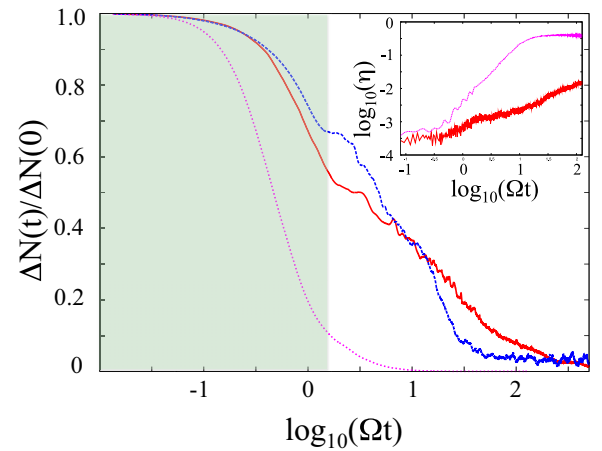


FIG. 4. (Color online) Inhomogeneity $\Delta N(t)$ as a function of Ωt for $\Omega/J = 0.013$, for $(n_D, n_S, L) = (2, 2, 20)$ (dashed blue) and $(3, 3, 27)$ (solid red). The results are obtained by exact diagonalization averaging over 50 and 25 random initial conditions, respectively. The shaded region indicates approximately the region of fast decay due to quasisonances. We depict for comparison the results for $(3, 3, 27)$ for $\Omega/J = 0.13$ (dotted pink). The inset shows the IPR for $(3, 3, 27)$ for $\Omega/J = 0.013$ (solid red) and $\Omega/J = 0.13$ (dotted pink).

(localized) state presents $\eta \sim 1$ ($\sim 1/n_{\max}$). Whereas for $\Omega/J = 0.13$, $\eta(t) \sim 1$ at $\Omega t < 10$, for $\Omega/J = 0.013$, $\eta(t)$ remains very small even for $\Omega t \gg 1$ (inset of Fig. 4), showing the appearance of quasilocalization in the many-body space.

g. Experimental feasibility. The previous scenarios can be realized with polar molecules in OLs, as we illustrate for the case of NaK, which possesses an electric dipole of 2.72 debyes in its lowest rovibrational level [48]. We consider the realistic case of partially polarized molecules with 1 debye. For a lattice spacing of 532 nm, $V/h \simeq 1$ kHz. Assuming a lattice depth of $18E_{\text{rec}}$, with $E_{\text{rec}}/h \simeq 2.75$ kHz the recoil energy, $J/h \simeq 10$ Hz = $|V|/100$, and hence $1/\Omega \sim 1$ s. As shown in Fig. 4 the slow dimer dynamics can be much larger, stretching well beyond a minute, which is the typical maximal lifetime in experiments. Localization can be explored either in expansion experiments, or by site-resolved measurements. Moreover, the formation of a repulsive gas with attractive DDI can be readily monitored. Tightening an overall harmonic trap should result in the formation of an incompressible crystalline core that can be revealed by measuring the saturation of the mean radius of the sample and/or by site-resolved measurements. Furthermore, BR hinders two or more molecules to gather

at the same site, preventing chemical recombination losses despite attractive DDI.

h. Summary. The absence of dissipation leads to rich out-of-equilibrium dynamics in polar lattice gases characterized by the formation of inter-site bound clusters and blockade repulsion even for attractive DDI. The combination of these effects with the control possibilities of ultracold gases may allow the realization of effective repulsive 1D gases with attractive DDI, the creation of dynamically bound crystals, and most interestingly, quasi-MBL in absence of disorder. The latter opens interesting perspectives for observing a dynamical phase transition in polar lattice gases from a delocalized to a quasi-MBL regime as a function of the V/J ratio.

Acknowledgments. We thank X. Deng, P. Naldesi, H. Weimer, and A. Zenesini for discussions. This work was supported by ERC (QGBE grant), Provincia Autonoma di Trento, Cariparo Foundation (Eccellenza Grant No. 11/12), Alexander von Humboldt foundation, MIUR (FIRB 2012, Grant No. RBFR12NLNA-002), cluster QUEST, and DFG Research Training Group 1729. L.B. thanks the CNR-INO BEC Center in Trento for CPU time. L.S. thanks the BEC Center in Trento for its hospitality.

-
- [1] A. Polkovnikov, K. Sengupta, A. Silva, and M. Vengalattore, *Rev. Mod. Phys.* **83**, 863 (2011).
- [2] See, e.g., M. A. Cazalilla, R. Citro, T. Giamarchi, E. Orignac, and M. Rigol, *Rev. Mod. Phys.* **83**, 1405 (2011), and references therein.
- [3] I. Bloch, J. Dalibard, and W. Zwerger, *Rev. Mod. Phys.* **80**, 885 (2008).
- [4] See, e.g., R. Nankishore and D. A. Huse, *Annu. Rev. Condens. Matter Phys.* **6**, 15 (2015), and references therein.
- [5] M. Schreiber, S. S. Hodgman, P. Bordia, H. P. Lüschen, M. H. Fischer, R. Vosk, E. Altman, U. Schneider, and I. Bloch, *Science* **349**, 842 (2015).
- [6] V. A. Mikheev, V. A. Mайдanov, and N. P. Mikhin, *Solid State Commun.* **48**, 361 (1983).
- [7] Yu. Kagan and L. A. Maksimov, *Zh. Eksp. Teor. Fiz.* **87**, 348 (1984) [*Sov. Phys. JETP* **60**, 201 (1984)].
- [8] G. Carleo, F. Becca, M. Schiró, and M. Fabrizio, *Sci. Rep.* **2**, 243 (2012).
- [9] M. Schiulaz and M. Müller, *AIP Conf. Proc.* **1610**, 11 (2014).
- [10] M. Schiulaz, A. Silva, and M. Müller, *Phys. Rev. B* **91**, 184202 (2015).
- [11] T. Grover and M. P. A. Fisher, *J. Stat. Mech.* (2014) P10010.
- [12] J. M. Hickey, S. Genway, and J. P. Garrahan, *arXiv:1405.5780*.
- [13] W. De Roeck and F. Huveneers, *Phys. Rev. B* **90**, 165137 (2014).
- [14] N. Y. Yao, C. R. Laumann, J. I. Cirac, M. D. Lukin, and J. E. Moore, *arXiv:1410.7407*.
- [15] Z. Papic, E. M. Stoudenmire, and Dmitry A. Abanin, *arXiv:1501.00477*.
- [16] A. Griesmaier, J. Werner, S. Hensler, J. Stuhler, and T. Pfau, *Phys. Rev. Lett.* **94**, 160401 (2005).
- [17] M. Lu, N. Q. Burdick, S. H. Youn, and B. L. Lev, *Phys. Rev. Lett.* **107**, 190401 (2011).
- [18] K. Aikawa, A. Frisch, M. Mark, S. Baier, A. Rietzler, R. Grimm, and F. Ferlaino, *Phys. Rev. Lett.* **108**, 210401 (2012).
- [19] K.-K. Ni *et al.*, *Science* **322**, 231 (2008).
- [20] C.-H. Wu, J. W. Park, P. Ahmadi, S. Will, and M. W. Zwierlein, *Phys. Rev. Lett.* **109**, 085301 (2012).
- [21] T. Takekoshi, L. Reichsöllner, A. Schindewolf, J. M. Hutson, C. R. Le Sueur, O. Dulieu, F. Ferlaino, R. Grimm, and H.-C. Nägerl, *Phys. Rev. Lett.* **113**, 205301 (2014).
- [22] See, e.g., T. Lahaye, C. Menotti, L. Santos, M. Lewenstein, and T. Pfau, *Rep. Prog. Phys.* **72**, 126401 (2009), and references therein.
- [23] See, e.g., M. A. Baranov, M. Dalmonte, G. Pupillo, and P. Zoller, *Chem. Rev.* **112**, 5012 (2012), and references therein.
- [24] B. Yan, S. A. Moses, B. Gadway, J. P. Covey, K. R. A. Hazzard, A. M. Rey, D. S. Jin, and J. Ye, *Nature (London)* **501**, 521 (2013).
- [25] A. de Paz, A. Sharma, A. Chotia, E. Maréchal, J. H. Huckans, P. Pedri, L. Santos, O. Gorceix, L. Vernac, and B. Laburthe-Tolra, *Phys. Rev. Lett.* **111**, 185305 (2013).
- [26] J. Hubbard, *Proc. Royal Soc. A* **276**, 238 (1963).
- [27] K. Winkler, G. Thalhammer, F. Lang, R. Grimm, J. Hecker-Denschlag, A. J. Daley, A. Kantian, H. P. Büchler, and P. Zoller, *Nature (London)* **441**, 853 (2006).
- [28] N. Strohmaier, D. Greif, R. Jördens, L. Tarruell, H. Moritz, T. Esslinger, R. Sensarma, D. Pekker, E. Altman, and E. Demler, *Phys. Rev. Lett.* **104**, 080401 (2010).
- [29] K. Góral, L. Santos, and M. Lewenstein, *Phys. Rev. Lett.* **88**, 170406 (2002).
- [30] In 1D a bound pair appears for any finite U , but unless $|U| \gg J$ the pair remains very delocalized. Only for $|U| \gg J$ a deeply bound on-site pair is formed.

- [31] M. J. Mark, E. Haller, K. Lauber, J. G. Danzl, A. Janisch, H. P. Büchler, A. J. Daley, and H.-C. Nägerl, *Phys. Rev. Lett.* **108**, 215302 (2012).
- [32] F. Heidrich-Meisner, S. R. Manmana, M. Rigol, A. Muramatsu, A. E. Feiguin, and E. Dagotto, *Phys. Rev. A* **80**, 041603(R) (2009).
- [33] J. P. Ronzheimer, M. Schreiber, S. Braun, S. S. Hodgman, S. Langer, I. P. McCulloch, F. Heidrich-Meisner, I. Bloch, and U. Schneider, *Phys. Rev. Lett.* **110**, 205301 (2013).
- [34] J.-P. Nguenang and S. Flach, *Phys. Rev. A* **80**, 015601 (2009).
- [35] M. Valiente, *Phys. Rev. A* **81**, 042102 (2010).
- [36] We used a maximal range of the DDI of $R_{NN} = 6$. Although this limits the maximal number of possible two-body bound states to $R_{NN} + 1$, it does not affect the results under the conditions we analyze.
- [37] Quantum deeply bound states differ from classical states of two particles at a fixed distance r only by a perturbative correction. If $f(r) \ll 1$ the probability to find the particles at a distance different than r is negligible. In practice, we may introduce a small $\epsilon = 0.01$ and define r_c such that $f(r_c) \lesssim \epsilon$ but $f(r_c + 1) \gg \epsilon$. For $V = -100J$ (Fig. 2) this criterion leads to $r_c = 2$.
- [38] Note that if $U = V$, a NN dimer resonates with an on-site pair. This allows the pair of particles to move resonantly along the lattice with the bare single-particle hopping.
- [39] This remains true for the formation of clusters of doubly occupied sites, which may be maintained in short-range interacting gases due to second-order processes [8].
- [40] J. F. Sherson, C. Weitenberg, M. Endres, M. Cheneau, I. Bloch, and S. Kuhr, *Nature (London)* **467**, 68 (2010).
- [41] S. R. White and A. E. Feiguin, *Phys. Rev. Lett.* **93**, 076401 (2004); A. E. Feiguin and S. R. White, *Phys. Rev. B* **72**, 020404(R) (2005).
- [42] Since by construction the maximal occupation per site is one, $\langle n_i^2 \rangle = \langle n_i \rangle$, and $g_2(t, r = 0) = \langle n_i \rangle^{-1}$. Hence, due to the homogenization of the density, $g_2(r = 0)$ quickly converges to the inverse density. For the case of Fig. 3(b) (4 particles in 24 sites), $g_2(r = 0) \rightarrow 6$.
- [43] G. E. Astrakharchik, D. Blume, S. Giorgini, and B. E. Granger, *Phys. Rev. Lett.* **92**, 030402 (2004); M. D. Girardeau and G. E. Astrakharchik, *ibid.* **109**, 235305 (2012).
- [44] See Supplemental Material at <http://link.aps.org/supplemental/10.1103/PhysRevB.92.180406> for a derivation of the effective model Eq. (2).
- [45] For $J_D = \Omega = 0$, immobile D's form effective box potentials, whose levels are occupied by the S's. For $J_D, \Omega > 0$, the motion of D's changes the energies of the box levels and the distribution of S's among them. As a result the energy of the system changes by an amount ΔE .
- [46] $\Omega/J = 0.13$ is considered just to illustrate better the localization for $\Omega/J \ll 1$ in model (2). Note that $\Omega/J = 0.13$ does not describe a polar gas at $V = -10J$, which has $r_c = 1$, and hence cannot be mapped to model (2).
- [47] Collective motion of two D's occurs in a time scale $\tau_2 \sim \Delta E/\Omega^2$, where ΔE is the typical energy shift when displacing one D. In our simulations $\Omega\tau_2 \simeq 10$. For the case of three D's the time scale for the collective motion is $\tau_3 \sim \Delta E^2/\Omega^3$, and hence $\Omega\tau_3 \simeq 100$ in good agreement with our results.
- [48] J. W. Park, S. A. Will, and M. W. Zwierlein, *Phys. Rev. Lett.* **114**, 205302 (2015).